# Reduction Potentials of $SO_3^{\bullet-}$, $SO_5^{\bullet-}$, and $S_4O_6^{\bullet 3-}$ Radicals in Aqueous Solution

**ARTICLE** *in* THE JOURNAL OF PHYSICAL CHEMISTRY A · APRIL 1999

Impact Factor: 2.69 · DOI: 10.1021/jp9900234



**3 AUTHORS**, INCLUDING:

Robert Huie
National Institute of Standards and Technolo…
**192** PUBLICATIONS **7,915** CITATIONS

SEE PROFILE

# Reduction Potentials of $SO_3^{\bullet-}$, $SO_5^{\bullet-}$, and $S_4O_6^{\bullet 3-}$ Radicals in Aqueous Solution

**Tomi Nath Das,† Robert E. Huie,* and P. Neta**

*Physical and Chemical Properties Division, National Institute of Standards and Technology, Gaithersburg, Maryland 20899-8381*

*Received: January 4, 1999; In Final Form: March 1, 1999*

Reduction potentials of the $SO_3^{\bullet-}$, $SO_5^{\bullet-}$, and $S_4O_6^{\bullet 3-}$ radicals in aqueous solutions are measured by pulse radiolysis at 294 K. These radicals are produced by reaction of $^{\bullet}OH$ or $N_3^{\bullet}$ radicals with sulfite, peroxymonosulfate, and thiosulfate anions, respectively. The potentials for the couples $SO_3^{\bullet-}/SO_3^{2-}$ and $SO_5^{\bullet-}/SO_5^{2-}$ are determined from equilibrium constants with three reference couples of the phenoxyl/phenoxide type, i.e., those derived from phenol, 3-cresol, and tyrosine. The potential for $PhO^{\bullet}/PhO^-$ is redetermined against $ClO_2^{\bullet}/ClO_2^-$ and confirms the published value. The potentials for the other two phenols are determined against $PhO^{\bullet}/PhO^-$. The potential for the $SO_3^{\bullet-}/SO_3^{2-}$ couple is found to be $0.73 \pm 0.01$ V vs NHE. The potential for $SO_5^{\bullet-}/SO_5^{2-}$ is found to be $0.81 \pm 0.02$ V. The reduction potential of the radical formed from the one-electron oxidation of thiosulfate, which exhibits a $\lambda_{max}$ at 375 nm, is also determined. This radical was identified before as either the monomeric $S_2O_3^{\bullet-}$ or the dimeric $S_4O_6^{\bullet 3-}$. Equilibrium measurements for this species, using $N_3^{\bullet}$ and the 4-cyanophenoxyl radical as references, support the dimeric assignment and yield a value of $1.07 \pm 0.03$ V for the reduction potential for the couple $S_4O_6^{\bullet 3-}/2S_2O_3^{2-}$.

## Introduction

**Radicals from Sulfite Autoxidation.** One hundred years ago, Bigelow presented an extensive study of the inhibitory effect of various organic compounds on the autoxidation of sulfite solutions.[1] Subsequent work by Young, Lumière, and Pinnow confirmed and extended these observations,[2−4] and a very important study by Titoff demonstrated the importance of trace metal catalysis.[5] Even earlier work by Jorissen had shown that the autoxidation of sulfite could induce the oxidation of other substances,[6] including transition metal ions.[7] Matthews and co-workers showed that the autoxidation reaction was accelerated greatly by ultraviolet light,[8] an effect that was inhibited by organic substances in the same manner as autoxidation in the dark.[9,10] Bäckström determined that the quantum yield of the photoinduced oxidation of sulfite was quite large.[11] He concluded that the thermal reaction was very similar to the photochemical reaction and, consequently, both reactions were chain reactions.[12] The autoxidation was also demonstrated to be initiated by α particles in a similar manner.[13] Haber then built upon this earlier information to propose a free radical mechanism, which has led us to that used today.[14] This free radical mechanism remained speculative until the early pulse radiolysis and flash photolysis studies of Hayon and co-workers that demonstrated the existence of the basic free radicals involved ($SO_3^{\bullet-}$ and $SO_5^{\bullet-}$) and began the process of unraveling their chemistry.[15,16]

Sulfite autoxidation is known to involve the $SO_3^{\bullet-}$, $SO_4^{\bullet-}$, and $SO_5^{\bullet-}$ radicals as intermediates and to be catalyzed by certain transition metal ions. The reaction may be initiated by the oxidation of sulfite by free radicals or transition metal ions (both represented here by $X^+$)

$$X^+ + SO_3^{2-} \rightarrow X + SO_3^{\bullet-} \quad (1)$$

$$SO_3^{\bullet-} + O_2 \rightarrow SO_5^{\bullet-} \quad (2)$$

Further, Connick and co-workers have suggested that the autoxidation of sulfite in the absence of transition metal ions involves the almost thermoneutral reaction[17]

$$HSO_5^- + HSO_3^- \rightarrow SO_4^{\bullet-} + SO_3^{\bullet-} + H_2O \quad (3)$$

In either case, the $SO_5^{\bullet-}$ and $SO_4^{\bullet-}$ radicals react further to propagate the chain

$$SO_5^{\bullet-} + X + H^+ \rightarrow X^+ + HSO_5^- \quad (4)$$

$$SO_5^{\bullet-} + SO_3^{2-} + H^+ \rightarrow HSO_5^- + SO_3^{\bullet-} \quad (5a)$$

$$SO_5^{\bullet-} + SO_3^{2-} \rightarrow SO_4^{2-} + SO_4^{\bullet-} \quad (5b)$$

$$SO_4^{\bullet-} + SO_3^{2-} \rightarrow SO_4^{2-} + SO_3^{\bullet-} \quad (6)$$

$$SO_5^{\bullet-} + SO_5^{\bullet-} \rightarrow 2SO_4^{\bullet-} + O_2 \quad (7)$$

or participate in termination reactions

$$SO_5^{\bullet-} + SO_5^{\bullet-} \rightarrow S_2O_8^{2-} + O_2$$

$$SO_3^{\bullet-} + SO_3^{\bullet-} \rightarrow S_2O_6^{2-} \quad (8)$$

When X is a transition metal ion, it may react with peroxymonosulfate, $HSO_5^-$, to branch the chain

$$X + HSO_5^- \rightarrow X^+ + OH^- + SO_4^{\bullet-} \quad (9)$$

The generation of these free radicals during the autoxidation of sulfite leads to many chemical and physiological conse-

* To whom correspondence should be addressed.

† On leave from the Chemistry Division, Bhabha Atomic Research Centre, Mumbai 400085, India.

10.1021/jp9900234 
Published on Web 04/22/1999

quences.[18,19] The rates of the reactions leading to these consequences are dependent largely on the reduction potentials of the various species involved. A recent study of DNA damage associated with sulfite autoxidation demonstrated that the details of the damage mechanisms depended intimately on the radical reduction potentials.[20] The $SO_4^{\bullet-}$ radical is known to be a very strong oxidant, with $E°$ ($SO_4^{\bullet-}/SO_4^{2-}$) = 2.43 V vs NHE[21] and, thus, can rapidly oxidize sulfite and many metal ions. The reduction potentials for $SO_3^{\bullet-}/SO_3^{2-}$ and for $SO_5^{\bullet-}/SO_5^{2-}$, however, are not well-established. A value for $SO_5^{\bullet-}/SO_5^{2-}$ of 1.1 V was estimated from kinetic measurements and may represent an upper limit.[22] Two reported values derived from pulse radiolysis studies for the $SO_3^{\bullet-}/SO_3^{2-}$ couple differ by almost 140 mV.[22,23] In the first study, chlorpromazine was the reference compound and there is some uncertainty in its reduction potential. In the second study, $ClO_2^{\bullet}$, which has a well-established potential, was the reference. But in this case, there is a question of whether the equilibrium involving sulfite and chlorite at high pH is reached via electron transfer only or whether it involves oxygen transfer as well.[24] To avoid this complication, the equilibrium constant for the reaction of $SO_3^{2-}$ with the tetraamine(phenanthroline)ruthenium(III) cation was derived from independent kinetic studies of the forward and reverse rate constants, specifically taking into consideration secondary reactions of $SO_3^{\bullet-}$.[25] In that work, the value $E°$ = 0.72 V was derived.

Because of these uncertainties in the potentials for $SO_3^{\bullet-}$ and $SO_5^{\bullet-}$, we have redetermined these reduction potentials in the present study. The reduction potentials were determined from equilibrium measurements, involving the $SO_3^{\bullet-}/SO_3^{2-}$ and $SO_5^{\bullet-}/SO_5^{2-}$ couples with several phenoxyl/phenoxide couples.

**Radicals from Thiosulfate.** In addition to $SO_3^{\bullet-}$ and $SO_5^{\bullet-}$, basic radicals of importance to sulfite oxidation, we have also measured reduction potentials for a radical derived from another oxyanion, thiosulfate $S_2O_3^{2-}$. Thiosulfate has been proposed as an oxidation inhibitor in flue gas desulfurization processes[26] and as an additive in spray solutions in nuclear power reactors, where it would react with volatile iodine.[27] Further, since the unpaired electron on the $S_2O_3^{\bullet-}$ radical is located on the terminal sulfur, there should be little structural difference between $S_2O_3^{2-}$ and $S_2O_3^{\bullet-}$, making this a convenient couple for studies of electron-transfer reactions.[28]

Adams and co-workers observed a transient spectrum centered about 375 nm after the pulse radiolysis of aqueous solutions of thiosulfate.[29] This spectrum, with $\epsilon$ = 1720 L mol$^{-1}$ cm$^{-1}$, was ascribed to the $S_2O_3^{\bullet-}$ radical, formed by the oxidation of $S_2O_3^{2-}$ by $^{\bullet}$OH.

$$^{\bullet}OH + S_2O_3^{2-} \rightarrow OH^- + S_2O_3^{\bullet-} \qquad (10)$$

The generation of this absorption in the flash photolysis of thiosulfate solutions was observed also by Dogliotti and Hayon[15]

$$S_2O_3^{2-} + h\nu \rightarrow S_2O_3^{\bullet-} + e_{aq}^- \qquad (11)$$

A second photolysis channel was thought to result in the generation of $^{\bullet}$OH and $S_2O_2^{\bullet-}$ but was demonstrated to be

$$S_2O_3^{2-} + h\nu \rightarrow SO_3^{\bullet-} + {}^{\bullet}S^- \qquad (12)$$

in a subsequent ESR (electron spin resonance) study by Behar and Fessenden.[30]

An absorption centered about 370 nm was also observed by Schöneshöfer after the pulse radiolysis of $N_2O$-saturated thiosulfate solutions.[31] Additional experiments demonstrated the same absorption feature in pulse radiolysis experiments, involving deaerated tetrathionate solutions containing formate, conditions that would favor one-electron reduction reactions

$$e_{aq}^- (CO_2^{\bullet-}) + S_4O_6^{2-} \rightarrow S_4O_6^{\bullet3-} + (CO_2) \qquad (13)$$

Therefore, it was proposed that the absorption at 370 nm in the photolysis and in the oxidation of thiosulfate arose from the reaction of the thiosulfate radical with thiosulfate to generate the dimer radical

$$S_2O_3^{\bullet-} + S_2O_3^{2-} \rightleftarrows S_4O_6^{\bullet3-} \qquad (14)$$

This interpretation was questioned by Mehnert and co-workers who studied the pulse radiolysis of thiosulfate and tetrathionate with greater time resolution.[27,32] In these studies, a very short lived absorption was observed at 320 nm, ascribed to the OH-thiosulfate adduct, which decays to another transient intermediate at 420 nm; this species is then transformed into the final form of the radical, absorbing at 370 nm. The authors explain these spectral changes by a reaction of the OH−thiosulfate adduct with an additional thiosulfate to generate a dimer absorbing at 420 nm. This dimer decomposes to the monomer radical that absorbs at 370 nm. This identification was based primarily on the ionic strength dependence of the self-reaction of the species absorbing at 370 nm.

To help resolve these discrepancies, we have reinvestigated the properties of the species absorbing at 375 nm, including a study leading to its reduction potential.

## Experimental Section[33]

**Materials.** Most of the compounds used were obtained from Aldrich, Alfa, and Mallinckrodt in their highest available purity (varying from 98% to >99%) and were used as received. Only *N*,*N*-dimethylaniline (DMA) was purified by refluxing and distilling over KOH under nitrogen. Sodium tetrathionate (>99%) was obtained from Fluka, sodium chlorite (80%) from Kodak, and potassium peroxymonosulfate as the triple salt Oxone ($2KHSO_5{\bullet}KHSO_4{\bullet}K_2SO_4$) from Aldrich. The content of $KHSO_5$ in the Oxone product was determined by adding excess $I^-$ and measuring the concentration of $I_3^-$ from its absorbance at 350 nm. It was found to correspond to 96% of the calculated value based on the above formula. Water was purified by a Millipore Super-Q system.

**Procedures.** To minimize thermal oxidation of the phenolic compounds by dissolved $O_2$ at high pH, all solutions were first saturated with $N_2O$ and then KOH was added to raise the pH to the desired level. Studies with peroxymonosulfate solutions indicate that this compound is thermally unstable at pH values near its second p$K_a$ (9.3) and rapidly evolves oxygen, but at higher pH values the $SO_5^{2-}$ ion is only moderately unstable and decomposes over a period of an hour (to ~5% of the starting value in the range of concentrations used in this study).[34] In our experiments, the concentration of $SO_5^{2-}$ in the alkaline solution was frequently checked by absorbance measurements during the progress of the study (about 15 min) and the corrected concentrations were used in the calculations. Additionally, to avoid any thermal reaction between $SO_5^{2-}$ and other reactants, these solutions were mixed just before entering the irradiation cell and the prepulse contact time was ≤2 s; therefore, any changes in the concentration of either reactant within this duration could be neglected.

The pulse radiolysis experiments were carried out in either one of two independent facilities, one based on a Febetron 705 pulser providing single 50 ns pulses of 2 MeV electrons and

**TABLE 1: Measurement of the Equilibrium Constant for $R^\bullet + S^- \rightleftarrows S^\bullet + R^-$**

| $S^\bullet$ | $[S^-]$ (mmol $L^{-1}$) | $R^\bullet$ | $[R^-]$ (mmol $L^{-1}$) | pH | $\lambda$ (nm) | added solute (mol $L^{-1}$) | $I$ | $K^a$ (mol $L^{-1}$) | $E°(I=0)^b$ (V) |
|---|---|---|---|---|---|---|---|---|---|
| $C_6H_5O^\bullet$ | 2 to 14 | $ClO_2^\bullet$ | 100 | 11.5 | 400 | | 0.120 | 213 ± 30 | 0.800 ± 0.005 |
| $TyrO^\bullet$ | 1.7 to 5.1 | $C_6H_5O^\bullet$ | 10 | 11.3 | 410 | $N_3^-$ (0.05) | 0.076 | 12.0 ± 1.2 | 0.736 ± 0.003 |
| $TyrO^{\bullet-}$ | 2.8 to 9.0 | $C_6H_5O^\bullet$ | 50 | 11.3 | 410 | $N_3^-$ (0.50) | 0.600 | 11.5 ± 1.2 | 0.737 ± 0.004 |
| $3\text{-}MeC_6H_4O^\bullet$ | 3.3 to 10.0 | $C_6H_5O^\bullet$ | 66 | 13 | 410 | | 0.100 | 12.4 ± 1.2 | 0.736 ± 0.003 |
| $DMA^{\bullet+}$ | 0.25 to 0.75 | $C_6H_5O^\bullet$ | 100 | 12 | 400 | glycol (2.7) | 0.180 | 69 ± 7 | 0.692 ± 0.003 |

[a] $K = ([R^-][S^\bullet])/([R^\bullet][S^-])$. [b] $E$ at zero ionic strength as explained in the text.

the other on a Varian linear accelerator providing multiple pulses of 5 MeV electrons with pulse duration of 50−500 ns. The detection in both systems is based on optical absorption in the UV and visible range. All measurements were carried out at room temperature, 21 ± 2 °C. Other experimental details were as described.[35]

**Calculation of Transient Equilibrium Constants.** In this work, equilibrium constants are determined, which involve two radicals that typically undergo subsequent radical−radical loss processes. Therefore, the experiments must be designed to establish the equilibrium among the reactants of interest on a time scale that is short when compared to the decay time due to radical−radical reactions. Further, it must be possible to determine the concentrations of all of the species involved in the equilibrium quantitatively. We will illustrate the procedures employed in this study with the following example: the equilibrium involving sulfite and a phenoxyl radical,

$$PhO^\bullet + SO_3^{2-} \rightleftarrows PhO^- + SO_3^{\bullet-} \quad (15)$$

The equilibrium constant for this reactions is given by

$$K_{eq} = \frac{[PhO^-][SO_3^{\bullet-}]}{[SO_3^{2-}][PhO^\bullet]} \quad (16)$$

which can be rearranged to:

$$\frac{[PhO^-]_{eq}}{[SO_3^{2-}]_{eq}} = \frac{[PhO^\bullet]_{eq}}{[SO_3^{\bullet-}]_{eq}} K_{eq} \quad (17)$$

The course of this reaction is followed by monitoring the phenoxyl radical, which is the only species in the system that absorbs in the visible portion of the spectrum (400 nm). In radiolysis experiments, the concentration of radicals produced is practically independent of the concentration of the solute, for low solute concentrations. The radicals arise only from the interaction of the radiation with the solvent.

$$H_2O \rightsquigarrow {}^\bullet OH + e_{aq}^- + H^+ \quad (+ \text{ small amounts of } H^\bullet, H_2, \text{ and } H_2O_2) \quad (18)$$

In these studies, the hydrated electron is converted to additional hydroxyl radicals by

$$e_{aq}^- + N_2O + H^+ \rightarrow {}^\bullet OH + N_2 \quad (19)$$

The initial phenoxyl and sulfite radicals then arise from the reactions of $^\bullet OH$ with $C_6H_5O^-$ and $SO_3^{2-}$

$$^\bullet OH + C_6H_5O^- \rightarrow OH^- + C_6H_5O^\bullet \quad (20)$$

$$^\bullet OH + SO_3^{2-} \rightarrow OH^- + SO_3^{\bullet-} \quad (21)$$

The total yield of radicals in any set of experiments at constant pulse intensity can be determined as the yield of phenoxyl radicals, $[PhO^\bullet]_o$, measured in the absence of added sulfite. In the presence of added sulfite, the concentration of sulfite radicals at equilibrium will be given by

$$[SO_3^{\bullet-}]_{eq} = [PhO^\bullet]_o - [PhO^\bullet]_{eq} \quad (22)$$

Also, in a pulse radiolysis experiment, the concentrations of the nonradical species are typically far greater than the concentrations of the radicals. Therefore, it is usually assumed that the equilibrium concentrations of the nonradicals are equal to the their initial concentrations. This assumption is not critical since corrections can be made easily if necessary.

The phenoxyl radical concentration is measured by its optical absorbance. In the absence of any sulfite, the absorbance is $A_o$; at equilibrium and in the presence of sulfite, the absorbance is $A_{eq}$. Since we are interested in the ratios of concentrations, the absolute values of the radical concentrations can be replaced by the phenoxyl radical absorbances. Thus:

$$\frac{[PhO^-]_o}{[SO_3^{2-}]_o} = \frac{A_{eq}}{A_o - A_{eq}} K_{eq} \quad (23)$$

This equation shows that the equilibrium constant can be derived from the slope of a plot of the ratio of the initial concentrations of phenoxyl and sulfite against the ratio of the equilibrium absorbance to the difference between the equilibrium absorbance and the absorbance measured in the absence of sulfite.

## Results and Discussion

**$SO_3^{\bullet-}$ and $SO_5^{\bullet-}$.** All equilibria were measured in alkaline solutions so that all the species are in their fully ionized forms. These reactions are typically faster than the equivalent reactions with neutral phenols, which also involve proton transfer. Choosing these conditions helps in attaining a rapid electron-transfer equilibrium at millimolar solute concentrations without a significant loss of radicals via other reactions. We set out to measure the equilibria for sulfite and peroxymonosulfate by using more than one reference compound and, as often as possible, by using the same reference compounds for both radicals. In view of the reported reduction potentials and following some preliminary measurements, we selected the three phenoxyl radicals derived from phenol, 3-cresol, and tyrosine as the most suitable for our purpose. The high self-exchange rates of these phenoxyl radicals was of advantage in helping to achieve rapid equilibration.[36]

As a first step, we redetermined the reduction potential of the phenoxyl/phenoxide couple against the well-accepted standard $ClO_2^\bullet/ClO_2^-$ ($E° = 0.934$ V vs NHE).[37]

$$ClO_2^\bullet + C_6H_5O^- \rightleftarrows ClO_2^- + C_6H_5O^\bullet \quad (24)$$

These measurements were carried out in $N_2O$ saturated solutions at pH 11.5, where >95% of the phenol is in the phenoxide form and the equilibrium was determined at the selected solute

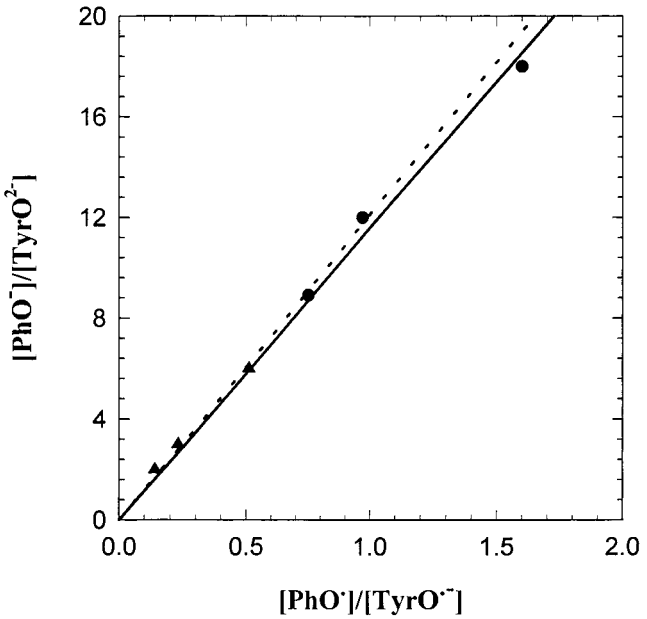


**Figure 1.** Measurement of the equilibrium constant for the reaction $C_6H_5O^\bullet + TyrO^{2-} \rightleftarrows C_6H_5O^- + TyrO^{\bullet -}$ at different ionic strengths, *I*, in $N_2O$ saturated solutions at pH 11.3, absorbed dose = 5.3 Gy per pulse. (•) $I = 0.6$ mol $L^{-1}$ with $[N_3^-] = 0.5$ mol $L^{-1}$, $[C_6H_5O^-] = 50$ mmol $L^{-1}$, $[TyrO^{2-}] = 2.8-9.0$ mmol $L^{-1}$ and (▲) $I = 0.076$ mol $L^{-1}$ with $[N_3^-] = 0.05$ mol $L^{-1}$, $[C_6H_5O^-] = 0.01$ mol $L^{-1}$, $[TyrO^{2-}] = 1.7-5.1$ mmol $L^{-1}$. Dashed line is the fit to the low ionic strength data; solid line is the fit to the high ionic strength data.

concentrations (Table 1). From the equilibrium constant, $K = 213 \pm 30$, we calculate $E^\circ = 0.80 \pm 0.01$ V vs NHE for the $C_6H_5O^\bullet/C_6H_5O^-$ couple, in excellent agreement with the value of 0.79 V reported earlier.[38] Our measured value is used as reference for all subsequent measurements on the sulfite and the peroxymonosulfate systems.

The second step in this process was to determine the reduction potentials of three other organic radicals against the phenoxyl/phenoxide couple. The three chosen were 3-methylphenoxyl/3-methylphenoxide (*m*-cresol), tyrosyl/tyrosine, and *N*,*N*-dimethylaniline radical cation/*N*,*N*-dimethylaniline. We measured the reduction potential of the phenoxyl radical derived from 3-cresol recently against phenol as the reference and found the value to be 0.736 V.[39] We include these results in Table 1. As part of the present study, we measured the equilibrium constant for the tyrosyl radical against phenol for subsequent use as reference in this study.

$$C_6H_5O^\bullet + TyrO^{2-} \rightleftarrows C_6H_5O^- + TyrO^{\bullet -} \qquad (25)$$

Tyrosine at pH 11.3 exists as the dianion; the tyrosyl radical is a monoanion. Therefore, we expected that the reverse reaction of equilibrium 25 would be dependent on ionic strength (*I*). The results at two different ionic strengths, however, clearly demonstrate (Table 1 and Figure 1) that the negative charge, localized on the carboxyl group at the side chain, does not affect significantly the reactivity of the radical center on the oxygen and the ring. The measured *K* values are 12 at $I = 0.07$ mol $L^{-1}$ and 11.5 at $I = 0.6$ mol $L^{-1}$. On the basis of these observations, the reduction potential for the tyrosyl radical has been assumed to be independent of ionic strength, $E = 0.736$ V.

The radical cation of *N*,*N*-dimethylaniline ($DMA^{\bullet +}$) was also selected as a reference for our estimations. However, because of the limited solubility of DMA in water, we used 2.7 mol $L^{-1}$ ethylene glycol solutions as the solvent matrix, where the oxidizing radical is $^\bullet CH_2CHO$.[40] At pH 12 and $I = 0.18$ mol $L^{-1}$, the equilibrium constant with phenol (reaction 26)

$$C_6H_5O^\bullet + DMA \rightleftarrows C_6H_5O^- + DMA^{\bullet +} \qquad (26)$$

was $K = 69$. Because the rate of the reverse reaction should be dependent on ionic strength, we corrected the measured value for the effect of ionic strength making use of an extended form of the Debye−Hückel equation:

$$\log K_{eq} = \log K_{eq}^\circ + 2Az_1z_2I^{1/2}/(1 + I^{1/2}) + \beta I \qquad (27)$$

where *I* is the ionic strength, $K_{eq}^\circ$ is the equilibrium constant at zero ionic strength, $z_i$ are the charges on the reactants, and *A* is a collection of physical constants with the value of 0.509 at 298 K.[41] The parameter $\beta$ is specific for each system and is normally obtained by experiment. Following Wardman,[42] we take $\beta = -0.02$. The value of *E* thus corrected to zero ionic strength for $DMA^{\bullet +}/DMA$ is 0.69 V. The reduction potentials for all the organic compounds used as references for the following studies are summarized in Table 1.

**Reduction Potential of the $SO_3^{\bullet -}/SO_3^{2-}$ Couple.** Equilibrium measurements for this couple with several reference systems are summarized in Table 2 and the data for tyrosine and cresol are shown in Figure 2. Studies with phenol were carried out at different ionic strengths and are presented in Figure 3, where the effect of the ionic strength on equilibrium 1 is clearly demonstrated. The *K* value decreases from 16.5 at $I = 0.067$ mol $L^{-1}$ to 9.23 at $I = 0.86$ mol $L^{-1}$. After correction to zero ionic strength, as described above, we calculated $E = 0.720$ V. With tyrosine (Figure 2a), the measurements at different ionic strengths once again confirmed that the negative charge on the carboxyl does not affect the equilibrium as much as would be predicted by the Debye−Hückel equation; the *K* value decreased marginally with increasing ionic strength from 0.61 at $I = 0.105$ mol $L^{-1}$ to 0.50 at $I = 0.3$ mol $L^{-1}$. The value of $E^\circ$ at zero ionic strength is estimated to be 0.736 V. With 3-cresol, the *K* value is 0.88 at $I = 0.08$ mol $L^{-1}$, giving $E^\circ = 0.733$ V at zero ionic strength. Measurements against DMA were not possible because of the limited solubility of this compound and the high

**TABLE 2: Measurement of $E(SO_3^{\bullet -})$ from the Equilibria $R^\bullet + SO_3^{2-} \rightleftarrows SO_3^{\bullet -} + R^-$**

| $[SO_3^{2-}]$ (mmol $L^{-1}$) | $R^\bullet$ | $[R^-]$ (mmol $L^{-1}$) | pH | $\lambda$ (nm) | added solute (mol $L^{-1}$) | *I* | *K* (mol $L^{-1}$) | $E(I = 0)^b$ (V) |
|---|---|---|---|---|---|---|---|---|
| 15 to 50 | $C_6H_5O^\bullet$ | 260 | 11.3 | 400 | KCl (0.50) | 0.855 | 9.23 ± 1.00 | 0.724 ± 0.002 |
| 4 to 12 | $C_6H_5O^\bullet$ | 50 | 11.6 | 400 | KCl (0.25) | 0.342 | 9.9 ± 1.0 | 0.724 ± 0.002 |
| 4 to 12 | $C_6H_5O^\bullet$ | 50 | 11.6 | 400 | KCl (0.10) | 0.192 | 10.6 ± 1.1 | 0.723 ± 0.003 |
| 4 to 12 | $C_6H_5O^\bullet$ | 50 | 11.6 | 400 | $K_2SO_4$[a] | 0.092 | 11.6 ± 1.2 | 0.724 ± 0.003 |
| 1.5 to 6.0 | $C_6H_5O^\bullet$ | 25 | 11.7 | 400 | $K_2SO_4$[a] | 0.067 | 16.54 ± 1.70 | 0.716 ± 0.005 |
| 40 to 60 | $TyrO^{\bullet -}$ | 5 to 15 | 12 | 410 | $K_3^-$ (0.20) | 0.300 | 0.50 ± 0.05 | 0.736 ± 0.003 |
| 10 to 30 | $TyrO^{\bullet -}$ | 10 | 11.5 | 410 | $K_2SO_4$[a] | 0.105 | 0.606 ± 0.035 | 0.736 ± 0.003 |
| 40 to 60 | 3-MeC6H4O• | 5 to 15 | 12 | 410 | $K_2SO_4$[a] | 0.080 | 0.88 ± 0.09 | 0.737 ± 0.004 |

[a] Added $K_2SO_4$ concentration maintained such that $[K_2SO_4] = [SO_3^{2-}]_{maximum} - [SO_3^{2-}]_{working}$.

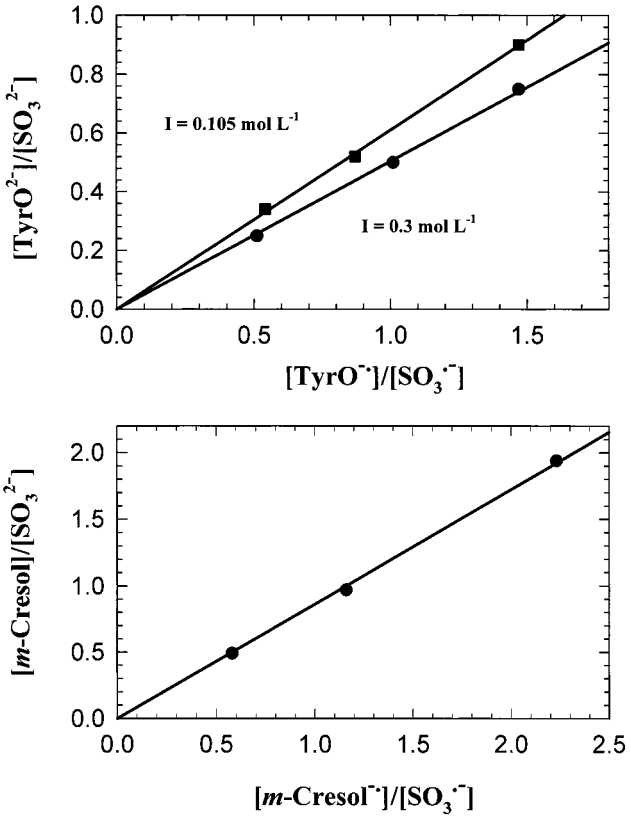


**Figure 2.** Measurement of the equilibrium constants for the reactions $TyrO^{\bullet} + SO_3^{2-} \rightleftarrows TyrO^- + SO_3^{\bullet-}$and $cresol^{\bullet} + SO_3^{2-} \rightleftarrows cresol^- + SO_3^{\bullet-}$.

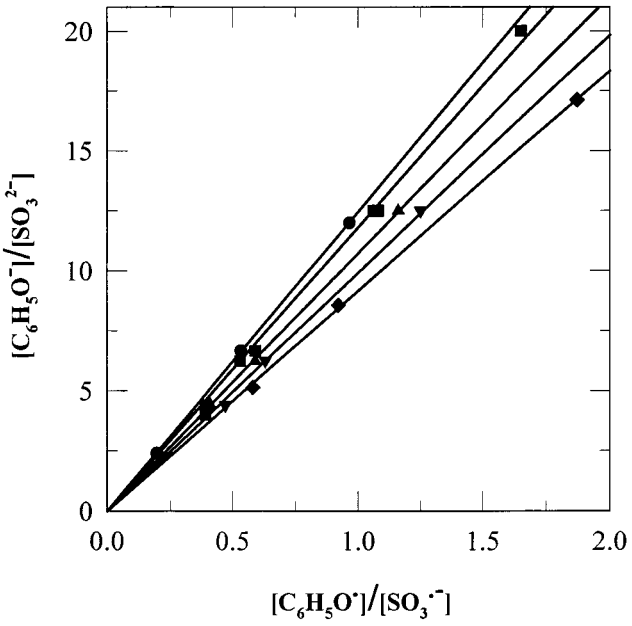


**Figure 3.** Variation of $K$ for the equilibrium between $C_6H_5O^{\bullet}/C_6H_5O^-$ and $SO_3^{\bullet-}/SO_3^{2-}$ in $N_2O$-saturated solutions at different $I$ values, absorbed dose ~5 Gy. The solution compositions for (•) $I = 67$ mmol $L^{-1}$, (■) $I = 92$ mmol $L^{-1}$, (▲) $I = 192$ mmol $L^{-1}$, (▼) $I = 342$ mmol $L^{-1}$, and (♦) $I = 855$ mmol $L^{-1}$ are listed in Table 2.

concentrations required for achieving equilibrium with sulfite before the radicals decay. From the three measurements summarized above, we calculate a reduction potential for the $SO_3^{\bullet-}/SO_3^{2-}$ couple at zero ionic strength of 0.73 ± 0.01 V vs NHE, where the estimated error limit represents the spread of the individual experimental values. The measurements leading to this value are summarized (along with similar measurements

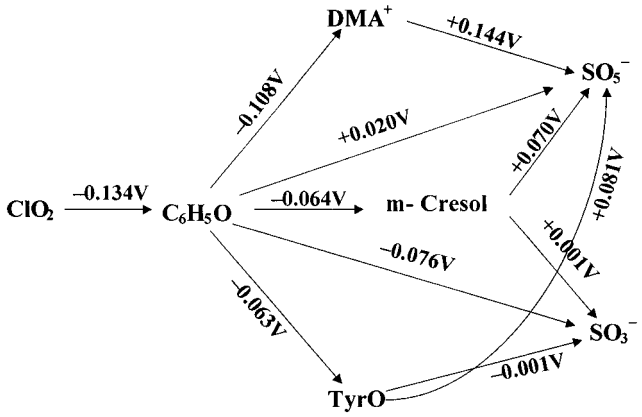


**Figure 4.** Redox relationships among the various species considered in this work in the derivation of the reduction potentials for $SO_3^{2-}$ and $SO_5^{2-}$. The numbers represent the reduction potential differences, going left to right, between the redox pairs.

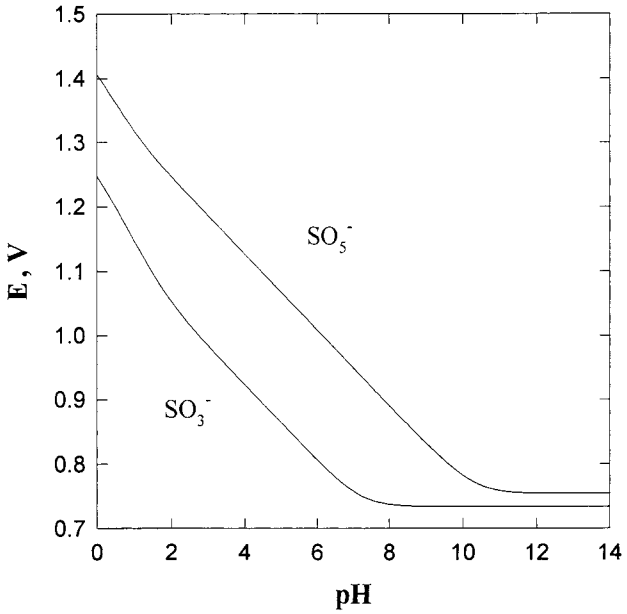


**Figure 5.** Reduction potentials for $SO_3^{\bullet-}/SO_3^{2-}$ and $SO_5^{\bullet-}/SO_5^{2-}$ as a function of the solution pH.

for $SO_5^{\bullet-}$) in Figure 4. Our value for the reduction potential of $SO_3^{\bullet-}$ is slightly lower than the value of 0.76 V measured against $ClO_2$[23] and higher than the value of 0.63 V measured against chlorpromazine,[22] but in good agreement with the value of 0.72 V derived from kinetic studies involving a ruthenium complex.[25]

From the value of $E = 0.73$ V for $SO_3^{\bullet-}/SO_3^{2-}$ at pH >11 we can calculate the reduction potential for the sulfite radical at other pH value by using eq 28.

$$E = E_0 + 0.059 \log(K_1K_2 + K_1[H^+] + [H^+]^2)/(K_r + [H^+]) \quad (28)$$

where $E_0$ is the reduction potential at pH 0. By taking the dissociation constants for sulfurous acid as $K_1 = 1.39 \times 10^{-2}$ and $K_2 = 6.3 \times 10^{-8}$ and assuming that the $SO_3^{\bullet-}$ radical does not protonate at pH > 2 ($K_r > 1 \times 10^{-2}$), we calculate the reduction potential at pH 7 to be $E_7 = 0.75$ V, at pH 4 $E_4 = 0.92$ V, and at pH 2 $E_2 = 1.04$ V vs NHE (Figure 5).

**Reduction Potential of the $SO_5^{\bullet-}/SO_5^{2-}$ Couple.** Equilibrium measurements for this couple were conducted at pH >11 since the rate of thermal decomposition of peroxymonosulfate

**TABLE 3: Measurement of $E(SO_5^{\bullet-})$ from the Equilibria $R^\bullet + SO_5^{2-} \rightleftarrows SO_5^{\bullet-} + R^-$**

| $[SO_5^{2-}]$ (mmol $L^{-1}$) | $R^\bullet$ | $[R^-]$ (mmol $L^{-1}$) | pH | $\lambda$ (nm) | $I^a$ (mol $L^{-1}$) | K | E°(I=0) (V) |
|---|---|---|---|---|---|---|---|
| 10 | $C_6H_5O^\bullet$ | 1 to 6 | 11.3 | 400 | 0.060 | $0.284 \pm 0.030$ | $0.820 \pm 0.005$ |
| 50 | 3-Me-$C_6H_4O^\bullet$ | 0.95 to 3.8 | 11.4 | 410 | 0.382 | $(3.7 \pm 0.4) \times 10^{-2}$ | $0.806 \pm 0.005$ |
| 50 | $TyrO^\bullet$ | 1 to 6 | 11.4 | 410 | 0.400 | $(2.1 \pm 0.2) \times 10^{-2}$ | $0.818 \pm 0.005$ |
| 15 to 25 | $DMA^{\bullet+}$ | 0.05 to 0.35 | 11 | 450 | 0.090 to 0.140 | $(3.7 \pm 0.4) \times 10^{-3}$ | $0.836 \pm 0.005$ |

[a] From $K_2SO_4$, equivalent of 1.5 times $[K_2SO_5]$ in the triple salt.

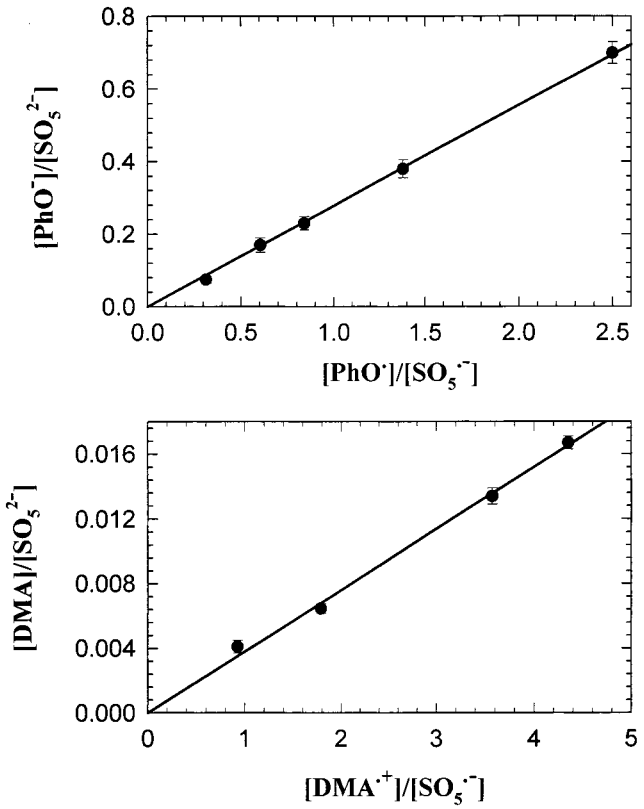


**Figure 6.** Measurement of the equilibrium constants for the reactions $PhO^\bullet + SO_5^{2-} \rightleftarrows PhO^- + SO_5^{\bullet-}$ and $DMA^{+\bullet} + SO_5^{2-} \rightleftarrows DMA + SO_5^{\bullet-}$.

is maximal near the second p$K_a$ value of 9.3 but is much slower at higher pH.[34,43] The results obtained with the four reference couples are summarized in Table 3. The $K$ value obtained with phenol as reference (Figure 6) was 0.284 at $I = 0.06$ mol $L^{-1}$. After correcting for the effect of ionic strength, we calculate $E = 0.820$ V. With tyrosine as reference, $K = 2.1 \times 10^{-2}$ at $I = 0.40$ mol $L^{-1}$, and the value of $E$ at zero ionic strength is 0.818 V. With 3-cresol, $K = 3.7 \times 10^{-2}$ at $I = 0.382$ mol $L^{-1}$, and the corrected $E$ is 0.806 V. With DMA as the reference (Figure 6), for $I$ between 0.09 and 0.14 mol $L^{-1}$, $K$ was $3.7 \times 10^{-3}$ and $E = 0.836$ V. The higher value in the latter case, as compared to the average value of $E° = 0.81 \pm 0.02$ V obtained with the three phenoxyl type references, is probably due to incomplete dissolution of the DMA added to the solutions containing Oxone. Therefore, the higher $E$ value of 0.836 is considered to be less certain and is not used in the final analysis, but the error limit quoted above has been expanded to include this value. The various measurements leading to the reduction potential of $SO_5^{\bullet-}$ are summarized in Figure 4.

From the average value of $E° = 0.81$ V for $SO_5^{\bullet-}/SO_5^{2-}$ at high pH and the p$K_a$ values for $H_2SO_5$ (1.0 and 9.3) and assuming that the $SO_5^-$ radical does not protonate at pH > 2, we calculate from eq 28 a reduction potential of $E_7 = 0.95$ V for $SO_5^{\bullet-}/HSO_5^-$ at pH 7, $E_4 = 1.12$ V at pH 4, and $E_2 = 1.24$ V at pH 2 (Figure 5).

In a recent pulse radiolysis study, the oxidation of $Mn^{2+}$ and its sulfite complexes by $SO_5^{\bullet-}$ radicals at pH 3 was reported to take place with a rate constant between $2 \times 10^8$ and $2 \times 10^{10}$ L $mol^{-1}$ $s^{-1}$ and to depend on the nature of the species being oxidized.[44] The standard reduction potential for the $Mn^{3+}/Mn^{2+}$ couple is 1.56 V vs NHE in strongly acidic solutions, where both ions are in their aquo form.[45] The aquo $Mn^{3+}$ ion is known to undergo stepwise deprotonation of its water molecules to form $Mn(OH)^{2+}$ and then $Mn(OH)^{2+}$, with p$K_a$ values of $-0.4$ and 0.3.[45] Therefore, at pH 3 the Mn(III) ion will exist as $Mn(OH)^{2+}$. From the p$K_a$ values and the reduction potential at high acidity, we estimate $E°$ (Mn(III)/$Mn^{2+}$) at pH 3 to be 1.19 V. From our results, $E°$ ($SO_5^{\bullet-}/SO_5^{2-}$) at pH 3 is 1.183 V. From this comparison of the reduction potentials it may be suggested that oxidation of Mn(II) at pH 3 by $SO_5^{\bullet-}$ radicals will have a relatively low rate constant. Since it is known that the nature of the complexing anion strongly affects the reduction potential of the Mn(III)/Mn(II) couple, we suggest that the high rate constants reported earlier[44] are probably due to reaction with the sulfite complex rather than with the aquo complex.

**Thiosulfate Radicals.** In our initial studies, we used the primary $^\bullet OH/^\bullet O^-$ radicals (p$K_a = 11.9$) and the secondary $N_3^\bullet$ radicals to react with thiosulfate. We observed symmetrical, broad absorption bands, an early one centered at $\lambda_{max}$ 420 nm and a later one centered at $\lambda_{max}$ 375 nm, in agreement with the absorption features reported in the literature. We then measured the rate constants for the oxidation of $S_2O_3^{2-}$ by several oxidizing radicals and found that while $Br_2^{\bullet-}$ reacts rapidly, with $k = (4.4 \pm 0.3) \times 10^8$ L $mol^{-1}$ $s^{-1}$, the reaction with $CO_3^{\bullet-}$ is slower by an order of magnitude, $k = (3.1 \pm 0.5) \times 10^7$ L $mol^{-1}$ $s^{-1}$, and $I_2^{\bullet-}$ is even less reactive, with $k \leq 10^6$ L $mol^{-1}$ $s^{-1}$. When $N_3^\bullet$ was used as the oxidant, it was observed that the maximum absorbance at 375 nm decreased with increasing $N_3^-$ concentration. This suggests that the reaction goes to equilibrium. Therefore, a systematic study was undertaken of this reaction. To achieve significant change in the yield of the thiosulfate radical, very high concentration ratios of $[N_3^-]/[S_2O_3^{2-}]$ were necessary. Thus, while the thiosulfate concentration was maintained in the range of several millimolar, the azide concentration was required to be in the range of several hundred millimolar. At these high azide concentrations, we had to take into account the dimerization equilibrium,

$$N_3^\bullet + N_3^- \rightleftarrows N_6^{\bullet-} \tag{29}$$

for which $K = 0.3$ L $mol^{-1}$ has been reported.[46,47]

The reaction was monitored at 375 nm, with a small correction for the absorbance due to $N_6^{\bullet-}$. The results were plotted by assuming an equilibrium involving $S_2O_3^{\bullet-}$

$$N_3^\bullet + S_2O_3^{2-} \rightleftarrows N_3^- + S_2O_3^{\bullet-} \tag{30}$$

or one involving the dimeric species.

$$N_3^\bullet + 2S_2O_3^{2-} \rightleftarrows N_3^- + (S_2O_3)_2^{\bullet3-} \tag{31}$$

**TABLE 4: Measurement of $E(S_4O_6^{\bullet 3-})$ from the Equilibria $R^\bullet + 2S_2O_3^{2-} \rightleftarrows (S_2O_3)_2^{\bullet 3-} + R^-$**

| $[S_2O_3^{2-}]$ (mmol $L^{-1}$) | $R^\bullet$ | $[R^-]$ (mmol $L^{-1}$) | pH | $\lambda$ (nm) | $I^a$ (mol $L^{-1}$) | $K$ | $E^\circ$ ($I = 0$) |
|---|---|---|---|---|---|---|---|
| 8 to 20 | $N_3^\bullet$ | 800 | 8.8 | 375 | 0.850 | $(2.0 \pm 0.2) \times 10^4$ | $1.054 \pm 0.003$ |
| 6 to 16 | $N_3^\bullet$ | 400 | 8.8 | 375 | 0.440 | $(1.9 \pm 0.2) \times 10^4$ | $1.060 \pm 0.004$ |
| 30 to 60 | 4-$CNC_6H_4O^\bullet$ | 20 | 12 | 375 | 0.280 | $2.2 \pm 0.2$ | $1.084 \pm 0.003$ |

[a] Added $K_2SO_4$ concentration maintained such that $[K_2SO_4] = [S_2O_3^{2-}]_{maximum} - [S_2O_3^{2-}]_{working}$.

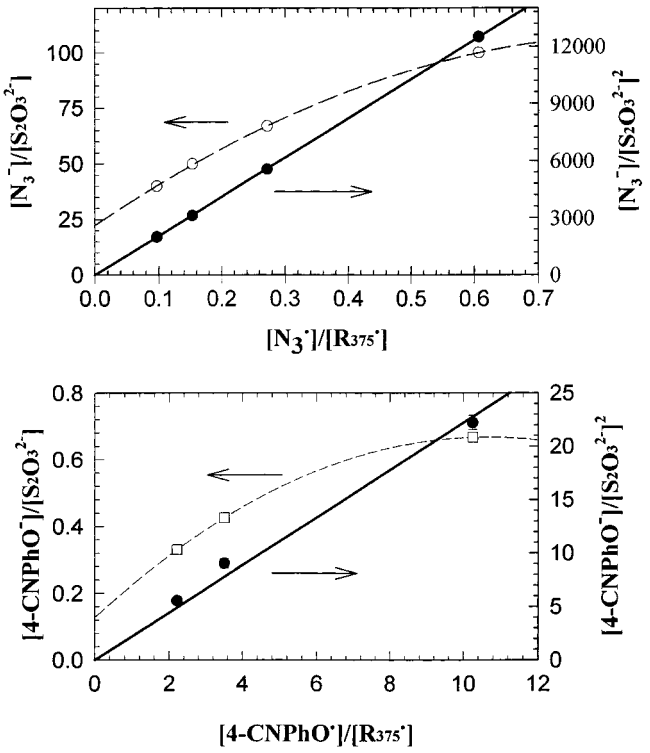


**Figure 7.** Equilibrium plots assuming monomeric and dimeric radicals from the oxidation of $S_2O_3^{2-}$ in $N_2O$-saturated solutions, absorbed dose 5−10 Gy. Solution compositions are presented in Table 4, (a) $N_3^\bullet$ as the oxidant and (b) 4-$CNC_6H_4O^\bullet$ as the oxidant.

The plots (Figure 7) indicate that if equilibrium 30 is assumed, the plot is strongly curved, whereas if equilibrium 31 is assumed to be valid, a straight line passing through the origin is obtained. For the latter case, the plot involves the square of the thiosulfate concentration,[21] i.e.

$$K = \frac{[N_3^-][(S_2O_3)_2^{3-}]}{[N_3^\bullet][S_2O_3^{2-}]^2} \qquad (32)$$

From the values $K = 2.0 \times 10^4$ (Table 4) at $I = 0.85$ mol $L^{-1}$ and $K = 1.9 \times 10^4$ at $I = 0.4$ mol $L^{-1}$ and taking $E = 1.35$ V for $N_3^\bullet/N_3^-$,[48] we calculate $E = 1.057$ V for the reduction potential of the $(S_2O_3)_2^{\bullet 3-}$ radical at zero ionic strength.

The value obtained for the reduction potential of the $(S_2O_3)_2^{\bullet 3-}$ radical is close to the reported reduction potential value of 1.12 V for the phenoxyl radical derived from 4-cyanophenol.[38] This prompted us to utilize this couple to verify the results relative to the $N_3^\bullet/N_3^-$ couple. As shown in Table 4 and Figure 7 at $I = 0.28$ mol $L^{-1}$, a value of $K = 2.2$ was obtained following similar arguments as in the case of azide above, and thus $E = 1.082$ V at zero ionic strength. The finding that in both experiments good linear plots are obtained when the equilibrium is assumed to involve the dimeric species suggests that the species absorbing at 375 nm has the dimeric structure. Combining the results of the two studies, we obtain $E^\circ = 1.07 \pm 0.03$ V for the reduction potential for $(S_2O_3)_2^{\bullet 3-}$, where the error limit is chosen to reflect the limited range of these studies. From this reduction potential and the estimated potential for the thiosulfate radical, $S_2O_3^{\bullet -}$, of $E^\circ = 1.30$ V,[49] we calculate $K_{eq} = 1.3 \times 10^{-4}$ L $mol^{-1}$ for the reaction

$$(S_2O_3)_2^{\bullet 3-} \rightleftarrows S_2O_3^{\bullet -} + S_2O_3^{2-} \qquad (33)$$

In an attempt to resolve the discrepancies in the assignment of the thiosulfate radical, we repeated some of the earlier experiments and compared the species formed by oxidation of thiosulfate with $^\bullet OH$ or $N_3^\bullet$ radicals with that formed by reduction of tetrathionate with $e_{aq}^-$. With solute concentrations above 5 mmol $L^{-1}$, both oxidation reactions with thiosulfate lead to the very rapid formation of a species with $\lambda_{max}$ at 420 nm and with $\epsilon = 4200 \pm 250$ L $mol^{-1}$ $cm^{-1}$. This species decays by first-order kinetics ($k_{obs} = (2 \pm 0.4) \times 10^6$ $s^{-1}$), independent of pH, solute concentration, dissolved $O_2$, or dose per pulse, to form the species absorbing with $\lambda_{max}$ 375 nm. These results are in agreement with those of Mehnert et al.,[27] except we did not observe the very short lived absorption at 320 nm under our conditions. The same 420 nm absorption is observed in the reduction of tetrathionate by $e_{aq}^-$, again in agreement with Mehnert et al. and supporting the identification of the absorption as from $S_4O_6^{\bullet 3-}$. In the oxidation reactions, this dimer results from the rapid reaction of excess $S_2O_3^{2-}$ with the initial oxidation product, possibly $S_2O_3^{\bullet -}$.

This leaves the question of the identity of the species absorbing at 375 nm. We find it difficult to accept that the dimeric species would rapidly decompose to its monomeric components, as suggested by Mehnert et al., since $S_2O_3^{\bullet -}$ radicals have been suggested to bind strongly to various other anions.[50] Moreover, our equilibrium measurements are in agreement with a dimeric structure for the radical absorbing at a $\lambda_{max}$ of 375 nm, not with a monomer. To rationalize these results, we suggest that the dimeric species absorbing at 420 nm, in which the binding involves four sulfur atoms in a row as in tetrathionate, i.e., $(^-O_3S-S-S-SO_3^-)^{\bullet -}$ rearranges rapidly to another dimeric species, possibly by breaking the central $(-S-S-)^{\bullet -}$ structure and forming an S−O bond instead, i.e., to form $(^-O_3S-S-O-SO_2-S^\bullet)^{2-}$. This rearrangement may take place via a four-centered cyclic intermediate. This suggested scheme satisfies the reaction kinetics reported earlier and those observed in our study. The absorption at 420 nm for the $(^-O_3S-S-S-SO_3^-)^{\bullet -}$ intermediate is similar to that of organic $(RS-SR)^{\bullet -}$ species. These species are known to be in equilibrium with their monomeric components and to monomerize at lower pH. The absorption at 375 nm suggested for the rearranged dimer is closer to that of monomeric $RS^\bullet$ radicals and thus is in line with a structure in which the radical is localized on one sulfur, as suggested.

**Acknowledgment.** We thank Dr. David Stanbury for helpful comments on this manuscript.

## References and Notes

(1) Bigelow, S. L. *Z. Phys. Chem.* **1898**, *26*, 493.
(2) Young, S. W. *J. Am. Chem. Soc.* **1902**, *24*, 297.
(3) Lumière, A.; Lumière, L.; Seyewetz, A. *Bull. Chem. Soc. Fr.* **1905**, *33*, 444.
(4) Pinnow, J. *Z. Electrochem.* **1913**, *19*, 262.

(5) Titoff, A. *Z. Phys. Chem.* **1903**, *45*, 641.
(6) Jorissen, W. P. *Z. Phys. Chem.* **1897**, *23*, 667.
(7) Jorissen, W. P. *Induced Oxidation*; Elsevier: Amsterdam, 1959.
(8) Matthews, J. H.; Dewey, L. H. *J. Phys. Chem.* **1913**, *17*, 211.
(9) Matthews, J. H.; Weeks, M. E. *J. Am. Chem. Soc.* **1917**, *39*, 635.
(10) Mason, R. B.; Mathews, J. H. *J. Phys. Chem.* **1926**, *30*, 414.
(11) Bäckström, H. L. J. *J. Am. Chem. Soc.* **1927**, *49*, 1460.
(12) Bäckström, H. L. J. *Z. Phys. Chem.* **1934**, *25B*, 122.
(13) Alyea, H. N. *J. Am. Chem. Soc.* **1930**, *52*, 2743.
(14) Haber, F. *Naturwissenschaften* **1931**, *19*, 450.
(15) Dogliotti, L.; Hayon, E. *J. Phys. Chem.* **1968**, *72*, 1800.
(16) Hayon, E.; Treinin, A.; Wilf, J. *J. Am. Chem. Soc.* **1972**, *94*, 47.
(17) Connick, R. E.; Zhang, Y. X.; Lee, S. Y.; Adamic, R.; Chieng, P. *Inorg. Chem.* **1995**, *34*, 4543.
(18) Neta, P.; Huie, R. E. *Environ. Health Perspect.* **1985**, *64*, 209.
(19) Huie, R. E. Chemical Kinetics of Intermediates in the Autoxidation of $SO_2$. In *Fossil Fuels Utilization: Environmental Concerns*; Markuszewski, R., Blaustein, B. D., Eds.; American Chemical Society: Miami Beach, FL, 1986; Vol. 319, p 284.
(20) Muller, J. G.; Hickerson, R. P.; Perez, R. J.; Burrows, C. J. *J. Am. Chem. Soc.* **1997**, *119*, 1501.
(21) Huie, R. E.; Clifton, C. L.; Neta, P. *Radiat. Phys. Chem.* **1991**, *38*, 477.
(22) Huie, R. E.; Neta, P. *J. Phys. Chem.* **1984**, *88*, 5665.
(23) Merényi, G.; Lind, J.; Shen, X. *J. Phys. Chem.* **1988**, *92*, 134.
(24) Suzuki, K.; Gordon, G. *Inorg. Chem.* **1978**, *17*, 3115.
(25) Sarala, R.; Islam, M. A.; Rabin, S. B.; Stanbury, D. M. *Inorg. Chem.* **1990**, *29*, 1133.
(26) Rochelle, G. T.; Owens, D. R.; Chang, J. C. S.; Brna, T. G. *J. Air Pollut. Control Assoc.* **1986**, *36*, 1138.
(27) Mehnert, R.; Brede, O.; Janovsky, I. *Radiat. Phys. Chem.* **1984**, *23*, 463.
(28) Sarala, R.; Stanbury, D. M. *Inorg. Chem.* **1992**, *31*, 2271.
(29) Adams, G. E.; Boag, J. W.; Michael, B. D. *Trans. Faraday Soc.* **1965**, *61*, 1674.
(30) Behar, D.; Fessenden, R. E. *J. Phys. Chem.* **1971**, *75*, 2752.
(31) Schöneshöfer, M. *Int. J. Radiat. Phys. Chem.* **1973**, *5*, 375.
(32) Mehnert, R.; Brede, O.; Janovsky, I. *Radiochem. Radioanl. Lett.* **1982**, *53*, 299.
(33) The identification of commercial equipment or materials does not imply recognition or endorsement by the National Institute of Standards and Technology nor does it imply that the material or equipment identified are necessarily the best available for the purpose.
(34) Marsh, C.; Edwards, J. O. *Prog. React. Kinet.* **1989**, *15*, 35.
(35) Das, T. N.; Dhanasekaran, T.; Alfassi, Z. B.; Neta, P. *J. Phys. Chem. A* **1998**, *102*, 280.
(36) Schuler, R. H.; Neta, P.; Zemel, H.; Fessenden, R. W. *J. Am. Chem. Soc.* **1976**, *98*, 3825.
(37) Stanbury, D. M. *Adv. Inorg. Chem.* **1989**, *33*, 69.
(38) Lind, L.; Shen, X.; Eriksen, T. E.; Merényi, G. *J. Am. Chem. Soc.* **1990**, *112*, 479.
(39) Das, T. N.; Neta, P. *J. Phys. Chem. A* **1998**, *102*, 7081.
(40) Steenken, S. *J. Phys. Chem.* **1979**, *83*, 595.
(41) Manov, G. G.; Bates, R. G.; Hamer, W. J.; Acree, S. F. *J. Am. Chem. Soc.* **1943**, *65*, 1765.
(42) Wardman, P. *J. Phys. Chem. Ref. Data* **1989**, *18*, 1637.
(43) Francis, R. C.; Zhang, X. Z.; Froass, P. M.; Tamer, O. *Tappi J.* **1994**, *77*, 133.
(44) Berglund, J.; Elding, L. I.; Buxton, G. V.; McGowan, S.; Salmon, G. A. *J. Chem. Soc., Faraday Trans.* **1994**, *90*, 3309.
(45) Biedermann, G.; Palombari, R. *Acta Chem. Scand.* **1978**, *A32*, 381.
(46) Butler, J.; Land, E. J.; Swallow, A. J.; Prütz, W. A. *Radiat. Phys. Chem.* **1984**, *23*, 265.
(47) Alfassi, Z. B.; Prütz, W. A.; Schuler, R. H. *J. Phys. Chem.* **1986**, *90*, 1198.
(48) Alfassi, Z. B.; Harriman, A.; Huie, R. E.; Mosseri, S.; Neta, P. *J. Phys. Chem.* **1987**, *91*, 2120.
(49) Sarala, R.; Rabin, S. B.; Stanbury, D. M. *Inorg. Chem.* **1991**, *30*, 3999.
(50) Schöneshöfer, M. *Ber. Bunsen-Ges. Phys. Chem.* **1973**, *77*, 257.